ELSEVIER

Journal of Materials Processing Technology 120 (2002) 355–364

Journal of Materials Processing Technology

www.elsevier.com/locate/jmatprotec

Induction heating process of an Al–Si aluminum alloy for semi-solid die casting and its resulting microstructure

H.K. Jung, C.G. Kang*

School of Mechanical Engineering, Engineering Research Center for Net Shape and Die Manufacturing (ERC/NSDM), Pusan National University, Pusan 609-735, South Korea

Accepted 10 September 2001

Abstract

During induction heating, the relationship between time and temperature must be controlled exactly to obtain a homogeneous temperature distribution over the entire cross-sectional area. Because the initial solid fraction in the semi-solid die casting (SDC) process is the main parameter to achieve a homogeneous flow behavior of the liquid and solid phases and to prevent macro-segregation effects in the SDC process, an accurately controllable induction heating method must be selected for the reheating process. The purpose of this work is not just to obtain the desire solid fraction, generally about 50%, but also to ensure the optimal induction heating conditions of A356 alloy to reduce the temperature gradient of a 76 mm diameter × 90 mm length billet and to obtain a fine globular microstructure without grain coarsening (resulting microstructure). This work shows that, in the case of a three-step reheating process for the SDC process, the final holding time is the most important factor to maintain a fine globular microstructure without grain coarsening.

Keywords: Induction heating process; Semi-solid die casting; Resulting microstructure; Solid fraction; Macro-segregation; Three-step reheating; Final holding time

1. Introduction

Semi-solid die casting (SDC) process of lightweight materials such as aluminum alloys, besides co-existing solid–liquid phases, is of increasing interest for manufacturing engineers and materials scientists [1–7]. This process clearly shows that semi-solid materials (SSMs) can be both thixotropic and pseudoplastic. A thixotropic material is one whose flow properties are time-dependent. This fact must be addressed, since many experimental investigations of SSM have been carried out under conditions different from those found in other metal forming processes.

Forming of materials in the semi-solid state includes both casting and deformation processes. The basic principle of this process is deformation at temperatures between solidus and liquidus points. However, the reheated billet has to be prepared before SDC, so that it has a very fine globular microstructure. To obtain the globular microstructure in a cross-section of the billet, optimal design of the induction coil is necessary [1–5].

In a study on the induction heating process of SSM, Kapranos et al. [3] compared numerical results with the temperature of five points in experiments with heating, soaking, and power-off stages. Sebus and Henneberger [6] proposed a new acoustic sensor system for determining the solid fraction of the reheated billet. Prikhodovsky et al. [7] simulated the microstructure evolution of aluminum alloys during isothermal holding at temperatures in the semi-solid range. Jung and Kang [1,5] proposed through the grain growth mechanism of Al–6%Si–3%Cu–0.3%Mg (ALTHIX 86S, this alloy is similar to ASM A319) alloy, solutions for avoiding coarsening phenomena during induction heating process and a new finite element numerical simulation model for the reheating process with an optimal coil design.

Most of relevant research that have been performed are about the properties of SSM, and none has been published on the overall effects of reheating parameters such as reheating time, billet size, and holding temperature on the resulting microstructure.

In this work, the optimal coil design to reduce the temperature gradient of the billet and to obtain the globular microstructure was theoretically proposed and tested by induction heating experiments. The effects of reheating time, holding temperature, holding time, adiabatic material

* Corresponding author. Tel.: +82-51-510-2335; fax: +82-51-512-1722.
E-mail addresses: hongkyuj@lycos.co.kr (H.K. Jung), cgkang@pusan.ac.kr (C.G. Kang).

0924-0136/02/$ – see front matter
PII: S0924-0136(01)01162-1

size, and capacity of the induction heating system on the resulting microstructure were considered.

2. Inductive coil design for uniform induction heating

For the SDC process, the reheating of the billet in the semi-solid state as quickly and homogeneously as possible is one of the most important parts of the process. From this point of view, the design of the induction coil is very important. For a real system consisting of coil and billet, the induced heat over the length of the billet is normally not equally distributed and consequently, there is a non-uniform temperature distribution. Therefore, an important point for optimization of coil design is to verify the correct relationship between coil length and billet length [1,5,8–10].

In this work, the optimal induction coil of a commercial 60 Hz induction heating system to obtain globular microstructure for variations of SSM and billet dimensions (diameter and length) was designed.

The optimal coil length H and coil inner diameter D_i of an induction heating system were designed for uniform reheating as shown in Fig. 1.

To consider the main surface power loss in induction heating, the idealized power density (P_s) must be represented as the actual power density (P_a), which is modified to allow for the ratio ($d/2\delta_F$) of the finite current depth of penetration (δ_F) of material and billet radius ($\frac{d}{2}$).

$$\delta_F = \sqrt{\frac{2\rho_a}{\mu w}} \tag{1}$$

$$P_a = \frac{P_s(\theta_s - \theta_c)_{\text{idealized}}}{\theta_s - \theta_c} = \frac{6.46k(\theta_s - \theta_c)}{d} \tag{2}$$

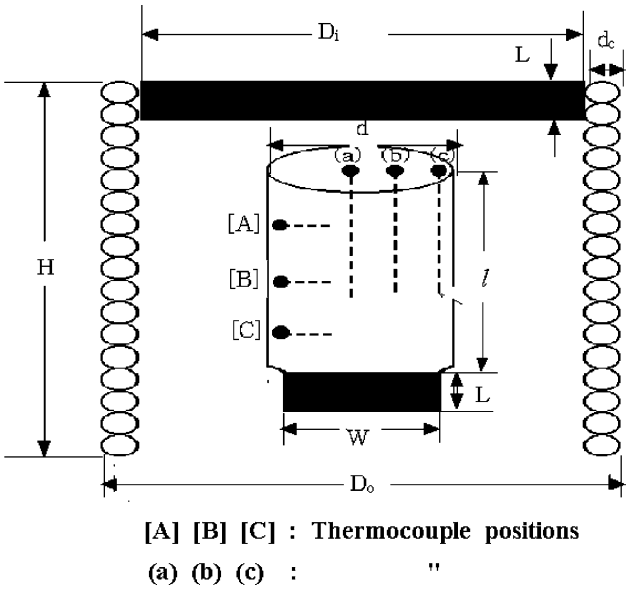

Fig. 1. Schematic diagram of induction heating system consisting of inductive coil and cylindrical billet.

Table 1
Recommended air gaps $[\frac{1}{2}(D_i - d)]$ for through-heating coils [11]

Frequency (Hz)	Billet temperature (°C)	Billet diameter, d (mm)		
		0–60	60–125	125–250
50/60	550	12	12	12
	850	12	20	40

In Eq. (2), $(\theta_s - \theta_c)/(\theta_s - \theta_c)_{\text{idealized}} = k$ can be obtained from the ratio ($d/2\delta_F$) of a finite current depth of penetration (δ_F) of material and billet radius ($\frac{d}{2}$) [11].

Here ρ_a, μ, ω, k, and $\theta_s - \theta_c$ are the resistivity of A356, the magnetic constant, the angular frequency, the thermal conductivity, and the maximum surface–center temperature difference, respectively.

If the production rate is assumed to be 10 billets heated per hour each 90 mm height, the temperature rises to 584 °C, because, by Stansel's data [12] (in the case of a temperature rise up to 510 °C, thermal capacity $q = 145\,\text{kW h/t}$, and production rate, $P_r = 0.01\,\text{t/h}$) and linear interpolation, the thermal capacity q and the production rate P_r are calculated. The minimum heated surface area A_s and the minimum heated length l_w can then be determined as follows:

$$A_s = \frac{P_t}{P_a} = \frac{P_r q}{P_a} \tag{3}$$

$$l_w = \frac{A_s}{\pi d} \tag{4}$$

To determine the coil inner diameter D_i and optimal coil length H, recommended air gaps $[\frac{1}{2}(D_i - d)]$ for through-heating coils and property values to calculate the optimal coil length are shown in Tables 1 and 2, respectively.

By using linear interpolation with Table 1, the coil inner diameter D_i is calculated, and from the result of Eq. (4), the optimal coil length H can be calculated by the following equation:

$$H = l_w + (25{-}75)\,\text{mm} \tag{5}$$

Therefore, from the above considerations, the proposed coil dimensions for the SSM with $d \times l = 76 \times 90\,(\text{mm}^2)$ are given in Table 3, and the experiments of induction heating were carried out by using those dimensions. The suitability of an optimal coil design was verified through the numerical simulation of the induction heating process by using ANSYS^{TM} [2,14]. From the results of the finite element numerical simulation, a coil length of 120 mm was most suitable to minimize the electro-magnetic end effect (under-heating or overheating of the billet).

3. Induction heating experiments for SDC

For the SDC process, the billet must be reheated to a semi-solid state. The reheating process is very important in the

Table 2
Property values used for the calculation of the optimal coil length ($f = 60$ Hz, $l = 90$ mm, $k = 0.62$)

Parameters	Symbol	Unit	Values	Ref.
Maximum surface–center temperature difference	$\theta_s - \theta_c$	K	4	
Current depth of penetration	δ	mm	10.7	[4]
Thermal conductivity	κ	W/m K	159	[13]
Idealized power density	P_s	kW/m^2	41.85	
Resistivity of A356	ρ_a	μΩ m	0.0421	[13]
Magnetic constant	μ	H/m	$4\pi \times 10^{-7}$	[11]
Angular frequency	ω	rad/s	120π	
Finite current depth of penetration	δ_F	m	1.3×10^{-2}	
Actual power density	P_a	kW/m^2	67.5	
Thermal power	P_t	kW	1.5	
Production rate	P_r	t/h	0.01	[12]
Thermal capacity	q	kW h/t	150	
Minimum heated surface area	A_s	m^2	22.2×10^{-3}	
Billet diameter	d	mm	76	
Minimum heated length	l_w	mm	93	

Table 3
Designed dimensions of induction coil ($f = 60$ Hz, $\delta = 10.7$ mm [4], $l = 90$ mm)

Billet diameter, d	Coil inner diameter, D_i	Minimum heating length, l_w	Optimal coil length, H
76 mm	100 mm	93 mm	118–168 mm

forming process of an SSM billet, it is necessary to achieve the required SSM billet state, and to control the microstructure of the billet.

The SSM used in this study was A356 alloys fabricated by electro-magnetic stirring, made by PECHINEY, France. This SSM is a casting alloy used in the manufacture of automotive parts. Its chemical composition is shown in Table 4, and the microstructure of the raw material is shown in Fig. 2. The primary crystal at as-cast microstructure fabricated by electro-magnetic stirring is not globular but similar to the equiaxed crystal. However, the primary crystal becomes globular when the raw material is remelted in the semi-solid condition.

Table 4
Chemical composition of A356 alloy (wt.%)

	Si	Fe	Cu	Mn	Mg	Cr	Zn	Ti	Pb
Minimum (%)	6.5	–	–	–	0.30	–	–	–	–
Maximum (%)	7.5	0.15	0.03	0.03	0.40	–	0.05	0.20	0.03

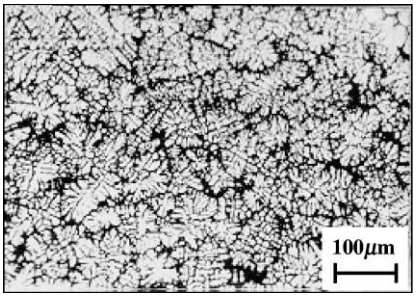

Fig. 2. Optical microstructure of as-cast raw A356 billet fabricated by electro-magnetic stirring in PECHINEY.

Billets of 76 mm × 90 mm were machined from the received A356 alloy. The induction heating experiments were performed by using an induction heating system with a capacity of 50 kW. As shown in Fig. 1, to achieve uniform heating, the heating coil of the induction heating system was made by machining to $D_o \times H = 120 \times 120\,(\text{mm}^2)$ [2,10,14]. Thermocouple holes to measure the temperature accurately are machined. To accurately control the temperature of the SSM, K-type CA thermocouples of ϕ1.6 mm are inserted into the billet. The thermocouples were calibrated against the boiling point of water. The accuracy of the thermocouples is approximately 0.2%. A data logger TDS-302 (Tokyo Sokki Kenkyuio) was used to receive the data, and the heating temperature was set to the datum as a thermocouple position b in Fig. 1.

To determine the optimal reheating conditions for the globularization of the microstructure and a small temperature gradient, the following parameters were considered: the capacity of the induction heating system (Q), reheating time (t_a), holding temperature (T_h), holding time (t_h), reheating steps, and adiabatic material size. The reheating experiments were performed for the conditions in Table 5. The meanings of the symbols used in Table 5 are the same as those shown in Fig. 3.

4. Results and discussion of induction heating experiments

The microstructure of SSM after reheating must be globular. Moreover, when the SSM is fed from the induction heating system to the die, the shape of the SSM must be maintained. Therefore, the capacity of the induction heating system (Q), reheating time (t_a), holding temperature (T_h),

Table 5
Induction heating conditions for the SDC using A356, test billet dimensions: $d \times l = 76 \times 90\,(\mathrm{mm}^2)$

Number	Relating time, t_a (min)			Holding temperature, T_h (°C)			Holding time, t_h (min)			Total time (min)	Capacity, Q (kW)	Adiabatic material size, $D \times W \times L$ (mm^3)
	t_{a1}	t_{a2}	t_{a3}	T_{h1}	T_{h2}	T_{h3}	t_{h1}	t_{h2}	t_{h3}			
1	4	4	2	350	575	584	1	3	2	16	3.00	Without
2	4	4	2	350	575	584	1	3	2	16	3.30	Without
3	4	4	2	350	575	584	1	3	2	16	4.94	Without
4	4	4	2	350	575	584	1	3	2	16	6.30	Without
5	4	4	2	350	575	584	1	3	2	16	7.00	Without
6	4	4	2	350	575	584	1	3	2	16	7.50	Without
7	4	4	2	350	575	584	1	3	2	16	7.796	Without
8	4	4	2	350	575	584	1	3	2	16	8.398	Without
9	4	4	2	350	575	584	1	3	2	16	8.398	$75 \times 70 \times 19$
10	10			584			2			12	7.796	$75 \times 70 \times 19$
11	10			584			2			12	8.398	$53 \times 53 \times 19$
12	8	1		575	584		3	2		14	8.398	$53 \times 53 \times 19$
13	4	3	1	350	575	584	1	3	2	14	8.398	$53 \times 53 \times 19$
14	4	3	1	350	575	584	1	3	1	13	8.398	$53 \times 53 \times 19$
15	4	3	2	350	575	584	1	2	1	13	8.398	$53 \times 53 \times 19$
16	4	3	2	350	560	584	1	3	1	14	8.398	$53 \times 53 \times 19$
17	4	3	2	350	560	584	1	2	2	14	8.398	$53 \times 53 \times 19$
18	3	3	2	350	565	584	1	3	2	14	8.398	$53 \times 53 \times 19$
19	4	4	2	350	565	584	1	3	2	16	8.398	$53 \times 53 \times 19$
20	4	3	1	350	575	584	1	3	3	15	8.398	$53 \times 53 \times 19$
21	4	4	2	350	575	584	1	3	2	16	8.398	$53 \times 53 \times 19$

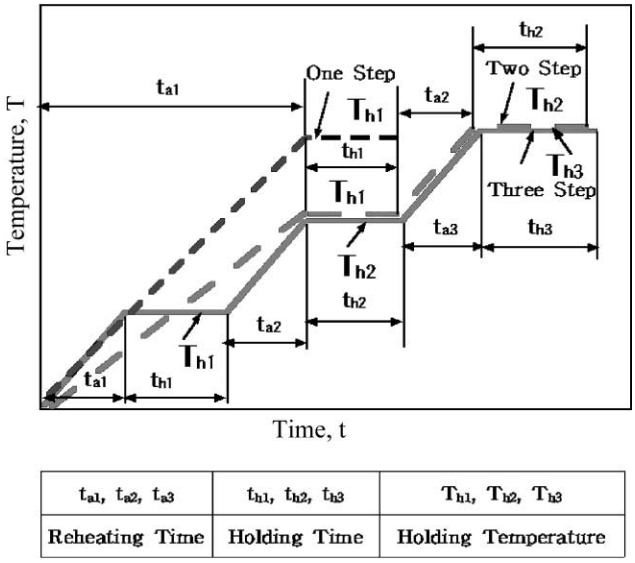

Fig. 3. Input data diagram of induction heating conditions to obtain the globular microstructure suitable for the SDC process.

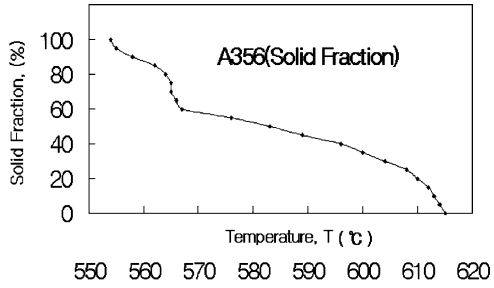

Fig. 4. Relationship between temperature and solid fraction for A356 (ALTHIX).

holding time (t_h), reheating steps, and adiabatic material size were considered as parameters of the experiment to observe the globularization of the microstructure and the temperature gradient.

The relationship between temperature and the solid fraction is given in Fig. 4. It can be seen that the solid fraction of ALTHIX changes rapidly at about 565 °C which is lower (up to 10 °C) than the eutectic remelting temperature of 575 °C [2,10,14,16]. According to the literature [15], the temperatures corresponding to the solid fraction of 50 and 55% are 584 and 576 °C, respectively.

For Exp. Nos. 1–21, the reheating experiments were performed for $f_S = 50\%$. For Exp. Nos. 1–9, the experiments were carried out at the reheating conditions $t_{a1} = 4\,\mathrm{min}$, $t_{a2} = 4\,\mathrm{min}$, $t_{a3} = 2\,\mathrm{min}$, $t_{h1} = 1\,\mathrm{min}$, $t_{h2} = 3\,\mathrm{min}$, $t_{h3} = 2\,\mathrm{min}$, $T_{h1} = 350\,°\mathrm{C}$, $T_{h2} = 575\,°\mathrm{C}$, and $T_{h3} = 584\,°\mathrm{C}$, but with a changing capacity of the induction heating system to determine the optimal capacity, by varying the heating time. In the case of the capacity (Q) of 7.796 and 8.398 kW, the billets reach the set temperature with a small temperature difference.

Therefore, Exp. Nos. 10 and 11 were performed under the conditions $t_{a1} = 10\,\mathrm{min}$, $t_{h1} = 2\,\mathrm{min}$, and $T_{h1} = 584\,°\mathrm{C}$, with the capacities ($Q$) of 7.796 and 8.398 kW. For Exp. Nos. 10 and 11, the sizes of adiabatic materials are $D \times W \times L = 75 \times 70 \times 19\,(\mathrm{mm}^3)$ and $D \times W \times L = 53 \times 53 \times 19\,(\mathrm{mm}^3)$, respectively. Figs. 5 and 6 show the

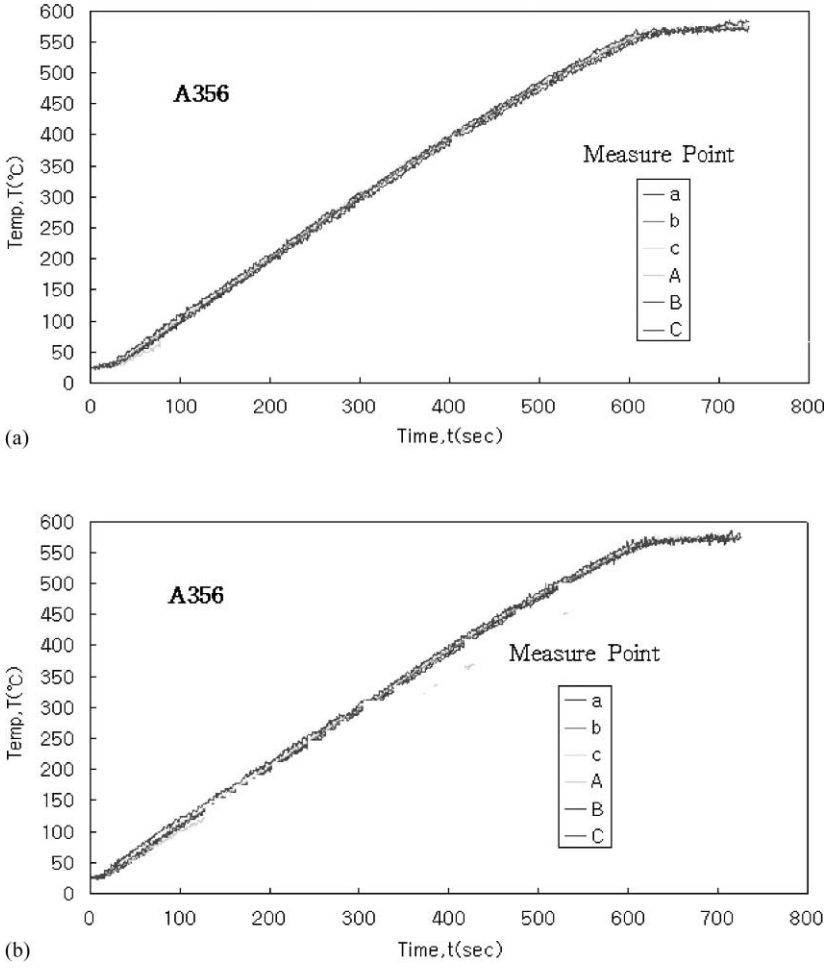

Fig. 5. Temperature distributions for different capacities of the induction heating system in one-step reheating process for SDC ($f_S = 50\%$, $t_{a1} = 10$ min, $T_{h1} = 584\,^{\circ}C$, $t_{h1} = 2$ min): (a) Exp. No. 10, $Q = 7.796$ kW; (b) Exp. No. 11, $Q = 8.398$ kW.

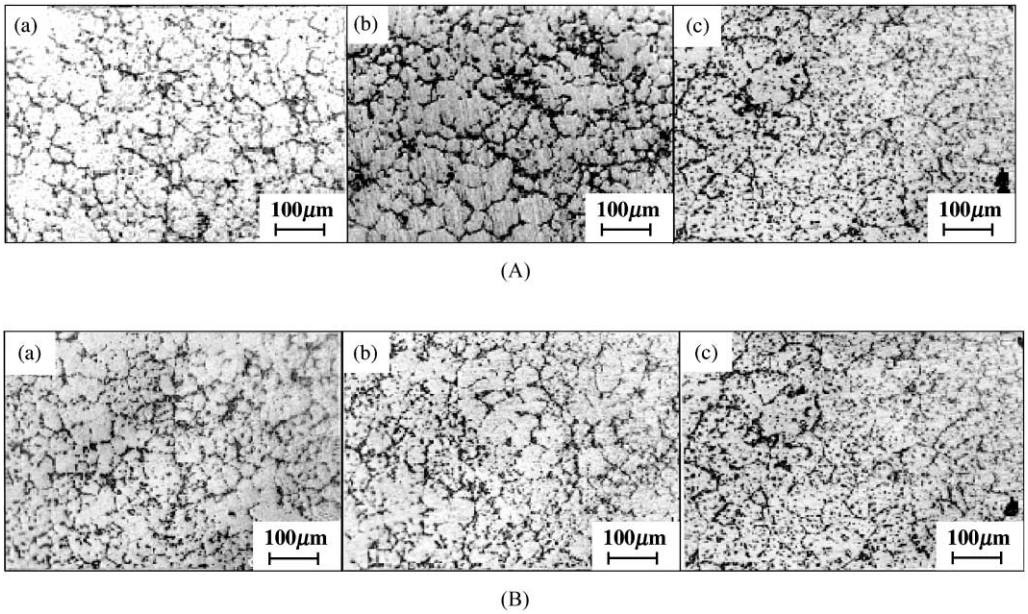

Fig. 6. Microstructure obtained in one-step reheating process for SDC with A356 ($f_S = 50\%$, $t_{a1} = 10$ min, $T_{h1} = 584\,^{\circ}C$, $t_{h1} = 2$ min): (A) Exp. No. 10, $Q = 7.796$ kW; (B) Exp. No. 11, $Q = 8.398$ kW.

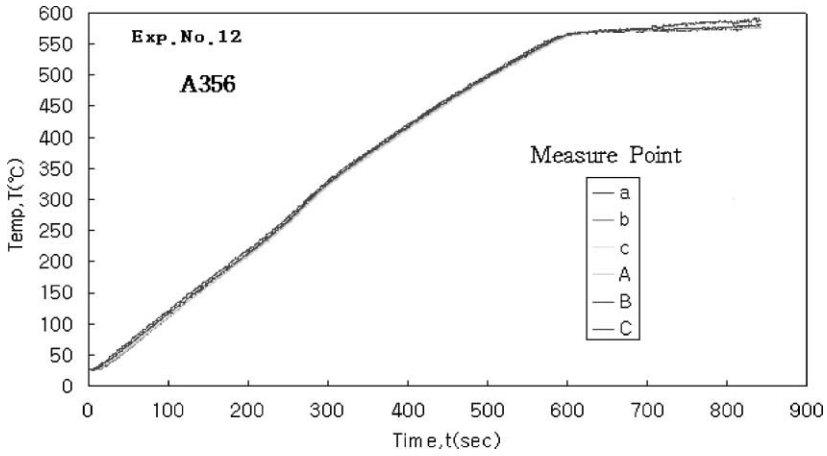

Fig. 7. Temperature distributions in two-step reheating process for SDC ($f_S = 50\%$, $t_{a1} = 8$ min, $t_{a2} = 1$ min, $T_{h1} = 575\,^{\circ}$C, $T_{h2} = 584\,^{\circ}$C, $t_{h1} = 3$ min, $t_{h2} = 2$ min, $Q = 8.398$ kW).

temperature distributions and microstructures of reheated SSM for Exp. Nos. 10 and 11. The temperature difference of the reheated SSM at the measured positions is small, the particle size is also generally small, but the globular microstructure is not obtained. Due to the lack of sufficient holding time for the separation between solid and liquid before and after the phase change, and for globularization of the solid particle, one-step reheating is unsuitable for the billet size of $d \times l = 76 \times 90\,(\text{mm}^2)$.

Exp. No. 12 was performed under the conditions $t_{a1} = 8$ min, $t_{a2} = 1$ min, $t_{a3} = 2$ min, $t_{h1} = 3$ min, $t_{h2} = 2$ min, $T_{h1} = 575\,^{\circ}$C, $T_{h2} = 584\,^{\circ}$C, and $Q = 8.398$ kW. Moreover, the size of the adiabatic material was $D \times W \times L = 53 \times 53 \times 19\,(\text{mm}^3)$. Figs. 7 and 8 show the temperature distribution and microstructure of the reheated SSM for Exp. No. 12. The temperature difference of the reheated SSM at the measured positions is small, and a good globular microstructure is obtained at positions a–c (Fig. 1). The degree of globularization is similar in positions a and b, but the microstructure of position c is coarse.

Exp. No. 13 was performed under the conditions $t_{a1} = 4$ min, $t_{a2} = 3$ min, $t_{a3} = 1$ min, $t_{h1} = 1$ min, $t_{h2} = 3$ min, $t_{h3} = 2$ min, $T_{h1} = 350\,^{\circ}$C, $T_{h2} = 575\,^{\circ}$C, $T_{h3} = 584\,^{\circ}$C, and $Q = 8.398$ kW. The size of the adiabatic material is $D \times W \times L = 53 \times 53 \times 19\,(\text{mm}^3)$. Figs. 9 and 10 show the temperature distribution and microstructure of reheated SSM for Exp. No. 13. The temperature difference of reheated SSM at the measured positions is small, and a fine globular microstructure is obtained at positions a–c (Fig. 1).

Comparing Exp. Nos. 12 and 13, the temperature difference of reheated SSM at the measured positions is small. The microstructure of Exp. No. 13 (three-step reheating) is finer and more globular than that of Exp. No. 12 (two-step reheating).

Exp. Nos. 14 and 20 were performed under the same conditions as Exp. No. 13, $t_{h3} = 1$ min and $t_{h3} = 3$ min, respectively. Figs. 9 and 10 show the temperature distributions and microstructures of the reheated SSM for Exp. Nos. 14, 13, and 20. The temperature difference of reheated SSM at the measured positions is small. For Exp. No. 14, the microstructure is not globular at positions a and b (Fig. 1), and the globularization is in progress at position c. Exp. No. 20 shows good globularization, but the size of the globularization is large at positions a–c (Fig. 1).

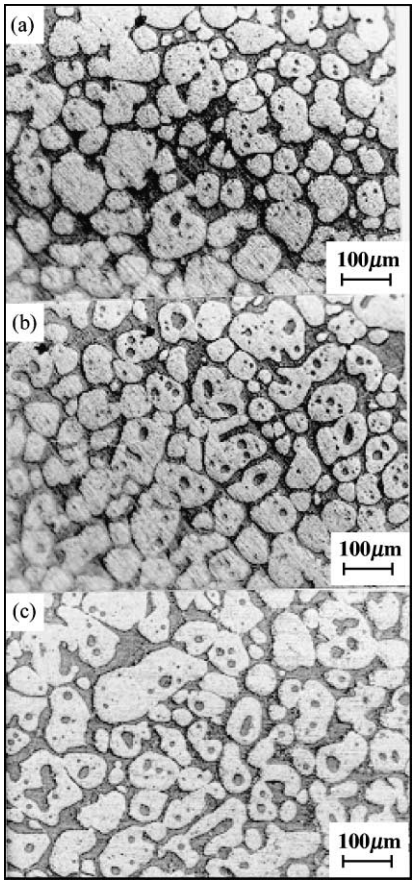

Fig. 8. Microstructure obtained in two-step reheating process for SDC with A356 (Exp. No. 12, $f_S = 50\%$, $t_{a1} = 8$ min, $t_{a2} = 1$ min, $T_{h1} = 575\,^{\circ}$C, $T_{h2} = 584\,^{\circ}$C, $t_{h1} = 3$ min, $t_{h2} = 2$ min, $Q = 8.398$ kW).

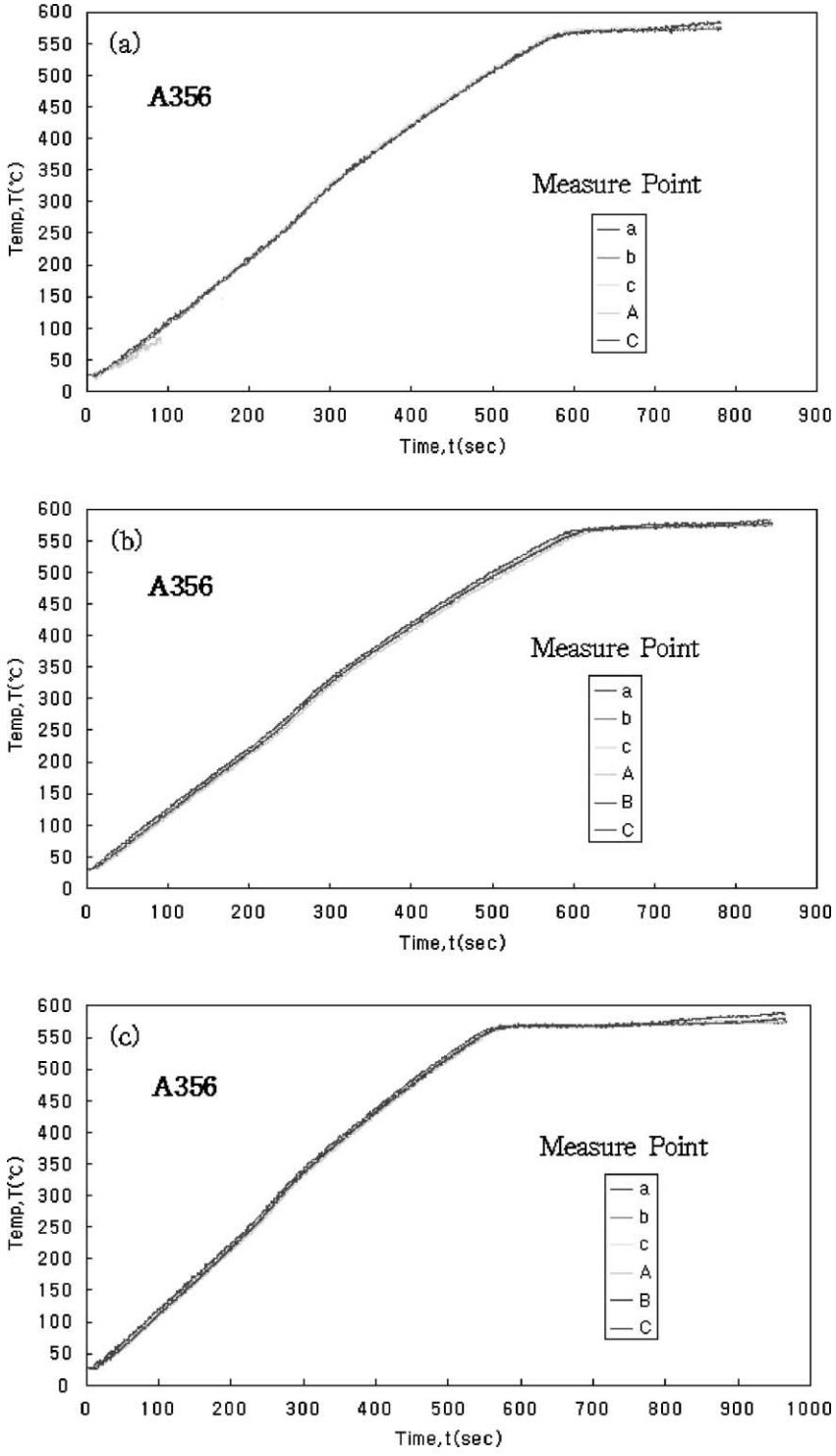

Fig. 9. Temperature distributions for the variation of t_{h3} in three-step reheating process for SDC ($f_S = 50\%$, $t_{a1} = 4$ min, $t_{a2} = 3$ min, $t_{a3} = 1$ min, $T_{h1} = 350\,^{\circ}C$, $T_{h2} = 575\,^{\circ}C$, $T_{h3} = 584\,^{\circ}C$, $t_{h1} = 1$ min, $t_{h2} = 3$ min, $Q = 8.398$ kW): (A) Exp. No. 14, $t_{h3} = 1$ min; (B) Exp. No. 13, $t_{h3} = 2$ min; (C) Exp. No. 20, $t_{h3} = 3$ min.

Exp. Nos. 19 and 21 were performed at $T_{h2} = 565\,^{\circ}C$ and $T_{h2} = 575\,^{\circ}C$. Figs. 11 and 12 show the temperature distributions and microstructures of reheated SSM for Exp. Nos. 19 and 21. In the case of Exp. No. 19, a globular microstructure was not obtained at position a (Fig. 1), globularization was in progress at position b, and a fine globular microstructure was observed at position c. In the case of Exp. No. 21, the temperature difference of the reheated SSM at the measured positions is larger than that of Exp. No. 19. Exp. No. 21 shows good globularization, but

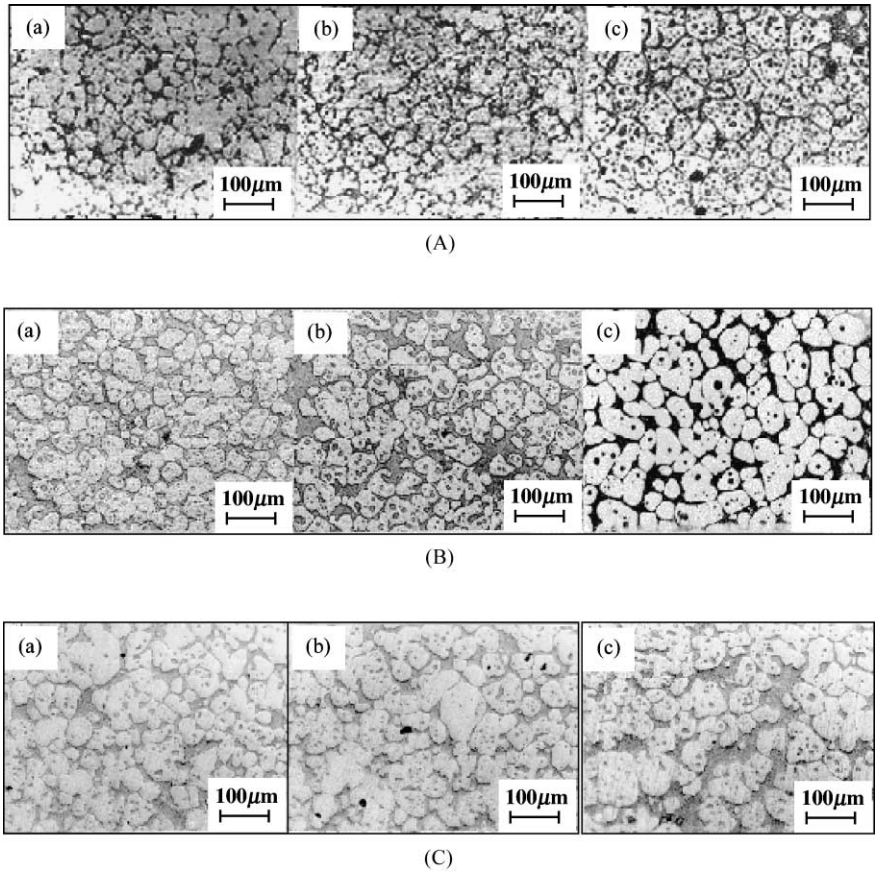

Fig. 10. Microstructure obtained in three-step reheating process for SDC with A356 ($f_S = 50\%$, $t_{a1} = 4$ min, $t_{a2} = 3$ min, $t_{a3} = 1$ min, $T_{h1} = 350\,^{\circ}$C, $T_{h2} = 575\,^{\circ}$C, $T_{h3} = 584\,^{\circ}$C, $t_{h1} = 1$ min, $t_{h2} = 3$ min, $Q = 8.398$ kW): (A) Exp. No. 14, $t_{h3} = 1$ min; (B) Exp. No. 13, $t_{h3} = 2$ min; (C) Exp. No. 20, $t_{h3} = 3$ min.

shows cohesion between solid regions at positions a–c (Fig. 1).

Fig. 13 shows the details of the eutectic microstructure of Exp. No. 13, which achieved the finest globular microstructure for $f_S = 50\%$. Fig. 13 shows that the eutectic is melted completely. Therefore, the A356 (ALTHIX) alloy is held without a change of temperature at around 575 °C, which is the eutectic temperature for 120–130 s. The solid fraction is then rapidly changed, because of the melting of the eutectic in this temperature range. It was found that the eutectic is melted completely at over 575 °C, and complete eutectic melting is necessary to obtain a fine globular microstructure. The temperature rise does not occur until sufficient thermal energy is provided to melt the eutectic, because much thermal energy and time are necessary to melt the eutectic [2,5,10,14]. Before and after the melting of the eutectic, the solid fraction is rapidly changed, and a rapid temperature rise occurs when the eutectic is melted. Due to this temperature rise, the temperature difference becomes large, and controlling the reheating temperature is difficult. Therefore, to homogeneously control the temperature distribution and the solid fraction of the SSM, the billet must be reheated in three-steps.

It was found that in the case of $d \times l = 76 \times 90\,(\mathrm{mm}^2)$ (shown in Fig. 10), one-step reheating is not a good process, because the size of the solid particles is small, and the globular microstructure is not obtained. As shown in Figs. 8, 10 and 12, three-step reheating is better than two-step reheating with respect to small solid particles and the accuracy of globularization.

The holding time of the final step is very important in the three-step reheating process [1,2,5,9,10,16,17]. As shown in Fig. 10(A), in the case of the three-step reheating process, if the holding time of the final step is short, the globular microstructure cannot be obtained, due to the lack of sufficient holding time for the separation between a solid and a liquid, before and after the phase change, and for globularization of the solid particles. On the other hand, if the holding time of the final step is too long, the risks of grain coarsening may be increased, due to the cohesion of the solid regions and the decrease in the liquid regions, as shown in Fig. 10(C). Therefore, the optimal holding time in the final step to obtain a fine globular microstructure without agglomeration is 2 min.

The proposed induction heating conditions with coil design enables the control of microstructure that affects the mechanical and rheological behavior [18–21] of alloys in the semi-solid state. In order to reduce the lead time for manufacturing, a study on the correlation between inductive

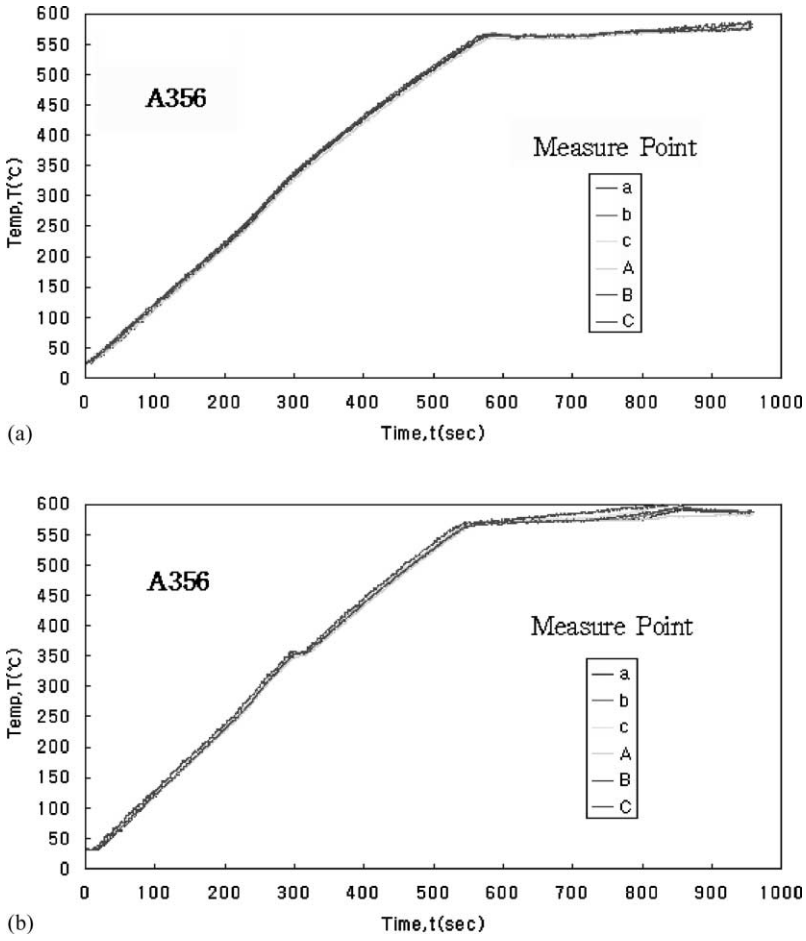

Fig. 11. Temperature distributions for the variation of T_{h2} in three-step reheating process for SDC ($f_S = 50\%$, $t_{a1} = 4$ min, $t_{a2} = 4$ min, $t_{a3} = 2$ min, $T_{h1} = 350\,^{\circ}$C, $T_{h3} = 584\,^{\circ}$C, $t_{h1} = 1$ min, $t_{h2} = 3$ min, $t_{h3} = 2$ min, $Q = 8.398$ kW): (a) Exp. No. 19, $T_{h2} = 565\,^{\circ}$C; (b) Exp. No. 21, $T_{h2} = 575\,^{\circ}$C.

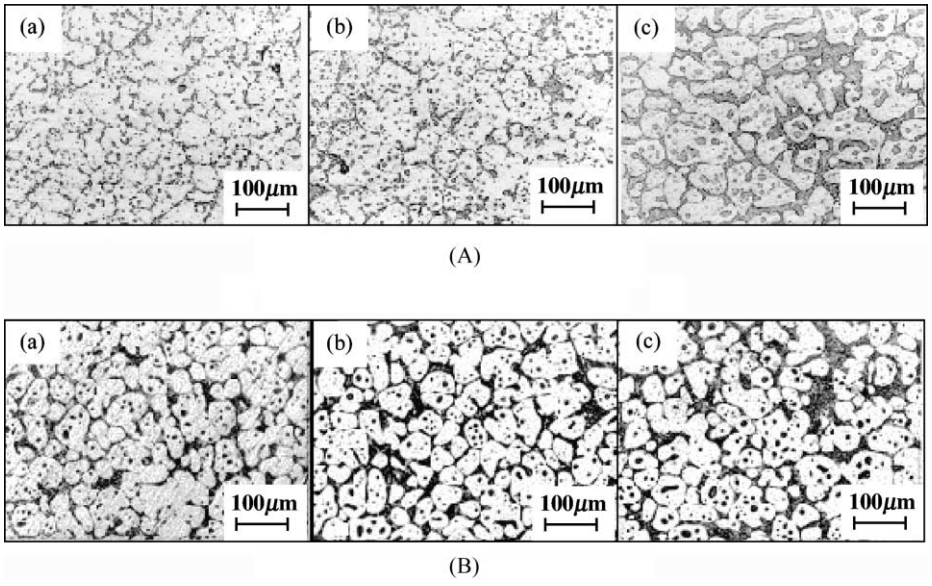

Fig. 12. Microstructure obtained in three-step reheating process for SDC with A356 ($f_S = 50\%$, $t_{a1} = 4$ min, $t_{a2} = 4$ min, $t_{a3} = 2$ min, $T_{h1} = 350\,^{\circ}$C, $T_{h3} = 584\,^{\circ}$C, $t_{h1} = 1$ min, $t_{h2} = 3$ min, $Q = 8.398$ kW): (A) Exp. No. 19, $T_{h2} = 565\,^{\circ}$C; (B) Exp. No. 21, $T_{h2} = 575\,^{\circ}$C.

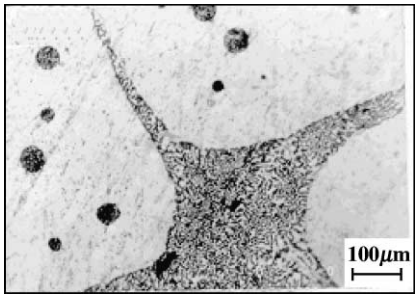

Fig. 13. Eutectic microstructure of A356 alloy in the semi-solid state (Exp. No. 13, $f_S = 50\%$, $t_{a1} = 4$ min, $t_{a2} = 3$ min, $t_{a3} = 1$ min, $T_{h1} = 350\,^{\circ}C$, $T_{h2} = 575\,^{\circ}C$, $T_{h3} = 584\,^{\circ}C$, $t_{h1} = 1$ min, $t_{h2} = 3$ min, $t_{h3} = 2$ min, $Q = 8.398$ kW).

heating modeling and final microstructures has been currently conducted.

5. Conclusions

To apply the SDC processes, the optimal coil design of A356 (ALTHIX) alloy with $d \times l = 76 \times 90\,(\mathrm{mm}^2)$ was theoretically proposed and tested by induction-heating experiments. In the reheating process of the A356 alloy with $d \times l = 76 \times 90\,(\mathrm{mm}^2)$, because the three-step reheating produces the best globular fine microstructure, it is more suitable than two-step reheating. The optimal holding time in the final step to obtain a fine globular microstructure without agglomeration is 2 min at the three-step reheating process.

Acknowledgements

Support for this work was provided by the Engineering Research Center for Net Shape and Die Manufacturing (ERC/NSDM), which is financed jointly by the Korea Science and Engineering Foundation (KOSEF). The authors want to express sincere gratitude to the ERC/NSDM and KOSEF for financial support during the course of this study.

References

[1] H.K. Jung, C.G. Kang, An induction heating process with coil design and solutions avoiding coarsening phenomena of Al–6%Si–3%Cu–0.3%Mg alloys for thixoforming, Metall. Mater. Trans. A 30 (11) (1999) 2967–2977.

[2] C.G. Kang, H.K. Jung, Y.J. Jung, Coil design of inductive heating and reheating process of aluminum alloys for thixoforming, Adv. Technol. Plast. 3 (1999) 1689–1694.

[3] P. Kapranos, R.C. Gibson, D.H. Kirkwood, C.M. Sellars, Induction heating and partial melting of high melting point thixoformable alloys, in: Proceedings of the Fourth International Conference on Semi-solid Processing of Alloys and Composites, The University of Sheffield, Sheffield, UK, 1996, pp. 148–152.

[4] V.I. Rudnev, L.C. Raymond, D.L. Loveless, M.R. Black, Induction Heat Treatment, Marcel Dekker, New York, 1997, pp. 775–911.

[5] H.K. Jung, C.G. Kang, Finite element numerical simulation modeling for reheating process of semi-solid forming, Key Eng. Mater. 177–180 (2000) 571–576.

[6] R. Sebus, G. Henneberger, Experiences using a band-coil and a new acoustic sensor system for inductive heating of aluminium alloys, in: Proceedings of the Sixth International Conference on Semi-solid Processing of Alloys and Composites (SSM2000), Unione Industriale di Torino, Turin, Italy, 2000, pp. 259–264.

[7] A. Prikhodovsky, I. Hurtado, D. Neuschutz, H. Gorgeneck, W. Bleck, Simulation and experimental investigations of microstructure coarsening of aluminium alloys, in: Proceedings of the Sixth International Conference on Semi-solid Processing of Alloys and Composites (SSM2000), Unione Industriale di Torino, Turin, Italy, 2000, pp. 521–526.

[8] C.G. Kang, H.K. Jung, A study on a thixoforming process using the thixotropic behavior of an aluminum alloy with an equiaxed microstructure, J. Mater. Eng. Perform. 9 (5) (2000) 530–535.

[9] H.K. Jung, C.G. Kang, Reheating process of cast and wrought aluminum alloys for thixoforging and their globularization mechanism, J. Mater. Process. Technol. 104 (3) (2000) 244–253.

[10] C.G. Kang, H.K. Jung, Semisolid forming process—numerical simulation and experimental study, Metall. Mater. Trans. B 32 (2) (2001) 363–372.

[11] E.J. Davies, Conduction and Induction Heating, Peter Peregrinus, London, 1990, pp. 100–222.

[12] N.R. Stansel, Induction Heating, McGraw-Hill, New York, 1949, p. 178.

[13] Metals Handbook, Properties and Selection: Nonferrous Alloys and Special-purpose Materials, Vol. 2, 10th Edition, ASM International, 1990, pp. 164–166.

[14] H.K. Jung, C.G. Kang, Finite element thermal analysis of induction heating process in hypoeutectic Al–Si materials for semi-solid forming, in: Proceedings of the Eighth International Symposium on Plasticity and Its Current Applications (PLASTICITY2000), Vancouver, BC, 2000, pp. 240–242.

[15] G. Hirt, R. Cremer, A. Winkelmann, T. Witulski, M. Zillgen, Semi-solid forming of aluminum alloys by direct forging and lateral extrusion, J. Mater. Process. Technol. 45 (1994) 359–364.

[16] M. Garat, S. Blais, C. Pluchon, W.R. Loué, Aluminium semi-solid processing: from the billet to the finished part, in: Proceedings of the Fifth International Conference on Semi-solid Processing of Alloys and Composites, Colorado School of Mines, Colorado, USA, 1998, pp. xvii–xxxi.

[17] J.C. Choi, H.J. Park, B.M. Kim, The influence of induction heating on the microstructure of A356 for semi-solid forging, J. Mater. Process. Technol. 87 (1999) 42–52.

[18] C.G. Kang, H.K. Jung, Finite element analysis with deformation behavior modelling of globular microstructure in forming process of semi-solid materials, Int. J. Mech. Sci. 41 (12) (1999) 1423–1445.

[19] H.K. Jung, C.G. Kang, Effect of alloying element on the mechanical behavior and superficial defects in thixoforged components of Al–Si alloys, Key Eng. Mater. 177–180 (2000) 565–570.

[20] N.S. Kim, H.K. Jung, C.G. Kang, A study on development of program for an automated thixoforming process design, J. Kor. Soc. Precis. Eng. 18 (1) (2001) 44–55.

[21] C.G. Kang, N.S. Kim, H.K. Jung, Automatic mesh generation and remeshing for finite element simulation of semi-solid forming process, in: Proceedings of the Sixth International Conference on Semi-solid Processing of Alloys and Composites (SSM2000), Unione Industriale di Torino, Turin, Italy, 2000, pp. 801–806.